33RD INTERNATIONAL COSMIC RAY CONFERENCE, RIO DE JANEIRO 2013
THE ASTROPARTICLE PHYSICS CONFERENCE

ICRC 2013

Measurement of the first harmonic modulation in the right ascension distribution of cosmic rays detected at the Pierre Auger Observatory: towards the detection of dipolar anisotropies over a wide energy range

IVÁN SIDELNIK[1] FOR THE PIERRE AUGER COLLABORATION[2]

[1] *Centro Atómico Bariloche and Instituto Balseiro (CNEA-UNCuyo-CONICET) and U.N. Río Negro, San Carlos de Bariloche, Argentina*
[2] *Full author list: http://www.auger.org/archive/authors_2013_05.html*

auger_spokespersons@fnal.gov

Abstract: First harmonic analyses of the right ascension distribution of cosmic rays detected at the Pierre Auger Observatory are reported. We here update the upper limits on the dipole component in the equatorial plane and extend the previous results to lower energies by using data recorded by the infill surface detector array. On the other hand, a possible consistency in ordered energy intervals of the phase was observed and reported, consistency that may be indicative of anisotropies whose amplitudes are too small to stand out above the background noise induced by the finite statistics accumulated so far. Based on this posterior observation, a prescribed single shot test was designed on June 25 2011 to establish at 99% CL whether this consistency is real or not. Since the effect has been observed over a wide energy range, the test makes use of data of both the infill and the regular surface detector arrays. At about mid-term, the status of this prescription is reported.

Keywords: Pierre Auger Observatory, ultra-high energy cosmic rays, large-scale anisotropies, first harmonic analysis.

1 Introduction

Large scale anisotropy studies are of major importance for cosmic ray physics, because together with the analysis of the spectrum and mass composition can help to understand the nature and origin of these particles. The measurement of the anisotropies at different energies, or the bounds on them, are relevant to constrain different models for the distribution of the sources and for the propagation of cosmic rays. For instance, the transition from a galactic to an extragalactic origin of the cosmic rays should induce a significant change in their large scale angular distribution and there are different theoretical models that locate this transition at different energies.

The Pierre Auger Observatory [1], located in Malargüe, Argentina, was originally designed to study the cosmic rays above 10^{18} eV. The Observatory combines two different techniques to detect the extensive air showers that are produced by the interactions of cosmic rays with the atmosphere. The surface detector array (SD) measures the lateral distribution of secondary particles at ground level and the fluorescence detector (FD) measures the longitudinal development of the air shower. The SD consists of an arrangement of 1600 water Cherenkov detectors distributed over an area of 3000 km^2 forming a triangular grid, with a detector separation of 1500 m, and has an operation duty cycle of nearly 100%. In order to enhance the capabilities of the Observatory by lowering its energy threshold a 23.5 km^2 area of the regular array has been deployed with detectors spaced by 750 m. This *infill* array [2] allows us to detect cosmic rays with energies down to 10^{16} eV and has full efficiency above 3×10^{17} eV.

We present in this work a study of the large scale distribution of arrival directions of cosmic rays based on the first harmonic analysis in right ascension with data from the surface detector of the Pierre Auger Observatory. An update of the search above 10^{18} eV as a function of both right ascension and declination is presented in [3]. Here we use for the first time the full energy range above 10^{16} eV. These energies are accessible thanks to the joint data acquired by both the infill array with 750 m spacing and the regular array with 1.5 km spacing. We use data up to the end of 2012, using events with zenith angles $\theta < 60^\circ$ for the 1.5 km spacing array, and $\theta < 55^\circ$ for the infill array.

2 First harmonic analysis in ordered energy intervals

2.1 Analysis method

Since the first harmonic modulations are quite small, it is important to account for possible spurious modulations of experimental or atmospheric origin or, alternatively, use methods which are not sensitive to these effects.

In particular, spurious variations due to the evolution of the array size with time or dead periods of each surface detector can be accounted by using the number of unitary cells $n_{cell}(t)$ recorded every second by the trigger system of the Observatory. The fiducial cut applied to the selected events [4] requires that the detector with the highest signal be surrounded by six active detectors, and hence the unitary cells that define the instantaneous exposure of the array to this type of events are defined as an active detector surrounded by six neighbouring active detectors. The same quality cut is used to select events recorded with the infill array. For any periodicity T, the total number of unitary cells $N_{cell}(t)$ summed over all periods, and its associated relative variations ΔN_{cell}, are obtained using:

$$N_{cell}(t) = \sum_j n_{cell}(t+jT), \quad \Delta N_{cell}(t) = \frac{N_{cell}}{\langle N_{cell}\rangle} \qquad (1)$$

with $\langle N_{cell}\rangle = 1/T \int_0^T dt N_{cell}$. To perform a first harmonic

analysis that accounts for the non-uniform exposure in different parts of the sky we introduce weights in the classical Rayleigh analysis. Each event is weighted with the inverse of the integrated number of unitary cells at the local sidereal time of the event. The Fourier coefficients a and b of the modified Rayleigh analysis are:

$$a = \frac{2}{\mathcal{N}} \sum_{i=1}^{N} w_i \cos(\alpha_i), \quad b = \frac{2}{\mathcal{N}} \sum_{i=1}^{N} w_i \sin(\alpha_i) \qquad (2)$$

where $w_i \equiv [\Delta N_{cell}(\alpha_i^0)]^{-1}$ with α_i^0 the local sidereal time of the event with right ascension α_i. We express α_i^0 in radians and chose it so that it is always equal to the right ascension of the zenith at the center of the array. The sum runs over the number N of events in the energy range considered, and $\mathcal{N} = \sum_{i=1}^{N} w_i$. The amplitude r and phase φ are calculated via $r = \sqrt{a^2 + b^2}$ and $\varphi = \arctan(b/a)$. They follow a Rayleigh and a uniform distributions, respectively, in the case of underlying isotropy.

Another source of systematic effects is induced by weather variations, leading both to daily and seasonal modulations. To eliminate these variations the conversion of the shower size into energy is performed by relating the observed shower size to the one that would have been measured at reference atmospheric conditions. Above 1 EeV, this procedure is sufficient to control the size of the sideband amplitude to the level of $\simeq 10^{-3}$ [5]. Below 1 EeV weather effects have a significant impact also on the detection efficiency for the regular array with 1.5 km spacing, and hence spurious variations of the counting rates are amplified. Therefore, we adopt in this case the differential *East* − *West* method [6]. This takes into account the difference between the event counting rate measured from the East sector, $I_E(\alpha^0)$, and the West sector $I_W(\alpha^0)$. Since the instantaneous exposure for Eastward and Westward events is the same, this difference allows us to remove, at first order in the direction, effects of experimental or atmospheric origin without applying any correction, although at the price of reducing the sensitivity to the first harmonic modulation. For the case of the infill, we will use only the East-West method since we are in this case particularly interested in the very low energies below full efficiency (while above 3×10^{17} eV the most sensitive results are obtained from the larger statistics accumulated by with the regular array with 1.5 km spacing). The amplitude r and phase φ can be calculated from the arrival times of N events using the standard first harmonic analysis slightly modified to account for the subtraction of the Western sector to the Eastern one. The Fourier coefficients a_{EW} and b_{EW} are defined by:

$$a_{EW} = \frac{2}{N} \sum_{i=1}^{N} \cos(\alpha_i^0 + \xi_i), \quad b_{EW} = \frac{2}{N} \sum_{i=1}^{N} \sin(\alpha_i^0 + \xi_i) \qquad (3)$$

where ξ_i=0 if the event comes from the East and $\xi_i = \pi$ if it comes from the West (in this way the events from the West are effectively subtracted). The amplitude r of the right ascension modulation determined with the Rayleigh formalism is related to $r_{EW} = \sqrt{a_{EW}^2 + b_{EW}^2}$ through the relation [5] $r = \frac{\pi \langle \cos(\delta) \rangle}{2 \langle \sin(\theta) \rangle} r_{EW}$. Note that the phase determined with the East-West method as $\varphi_{EW} = \arctan(b_{EW}/a_{EW})$ is related to the phase determined with the Rayleigh formalism by $\varphi = \varphi_{EW} + \pi/2$.

2.2 Analysis at the sidereal frequency

To perform first harmonic analyses as a function of energy, the choice of the size of the energy bins is important to avoid the dilution of a genuine signal with the background noise. The size of the energy bins for the analysis with the array with 1.5 km spacing was chosen to be $\Delta \log_{10}(E) = 0.3$ below 8 EeV (and one single bin for all energies above 8 EeV was used). This is larger than the energy resolution. For the analysis with the infill array a bin size of $\Delta \log_{10}(E) = 0.6$ was used. Data from the larger array was used for energies above 0.25 EeV, and the infill array was used to complement this measurements down to 0.01 EeV.

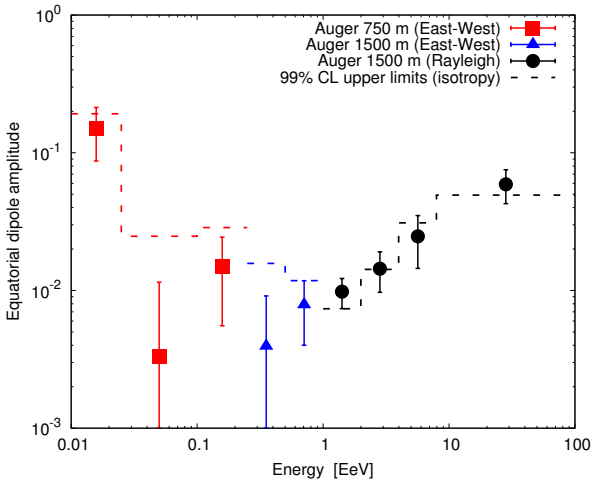

Figure 1: Equatorial dipole amplitude as a function of energy. The results of the modified Rayleigh analysis are shown with black circles and blue triangles corresponds to the analysis with East-West method, in both cases using data from the array with 1.5 km spacing. Red squares correspond to data from the infill array using the East-West method. The dashed lines are the 99% CL upper values of the amplitude that could result from fluctuations of an isotropic distribution.

The Rayleigh amplitude r measured by any observatory can be used to reveal (or infer) anisotropies projected on the Earth equatorial plane. In the case of an underlying pure dipole, the relationship between r and the projection of the dipole on the Earth equatorial plane, $d_\perp$, depends on the latitude of the observatory and on the range of zenith angles considered : $d_\perp \simeq r / \langle \cos \delta \rangle$ [5]. $d_\perp$ is the physical quantity of interest to compare the results of different experiments and the pure dipole predictions. For the regular array one has that $\langle \cos \delta \rangle \simeq 0.78$ while for the infill this number results $\langle \cos \delta \rangle \simeq 0.79$. The obtained amplitude $d_\perp$ is shown in Fig. 1 and in Table 1, the dashed line in the plot represents the upper values of the amplitude which may arise from fluctuations in an isotropic distribution at 99% CL, denoted by $d_{\perp 99\%}^{iso}$. Table 1 shows also the number of events, N, the phase with its associated uncertainty, the probability P that an amplitude larger or equal than that observed in the data arises by chance from an isotropic distribution ($P(> r) = \exp(-r^2 \mathcal{N}/4)$).

Note that in the energy ranges 1-2 and 2-4 EeV the measured amplitudes of $d_\perp$ of $(1.0 \pm 0.2)\%$ and $(1.4 \pm 0.5)\%$ have a probability to arise by chance from an isotropic distribution of about 0.03% and 0.9%, while above 8 EeV the measured amplitude of $(5.9 \pm 1.6)\%$ has chance probabil-

	ΔE[EeV]	N	$d_\perp \pm \sigma_{d_\perp}$ [%]	$\varphi \pm \Delta_\varphi$ [°]	P($> d_\perp$) [%]	$d^{iso}_{\perp 99\%}$ [%]	$d^{ul}_\perp$ [%]
Infill	0.01 - 0.025	11819	15 ±6.3	334± 25	5.9	19	28.6
East-West	0.025 - 0.1	428028	0.3±0.8	122±180	92	2.4	2.2
Method	0.1 - 0.25	223342	1.4±0.9	277± 39	28	2.9	3.5
East-West	0.25 - 0.5	720224	0.4±0.5	280±180	75	1.6	1.5
Method	0.5 - 1	1081810	0.8±0.4	258± 30	13	1.2	1.6
	1 - 2	557829	1.0±0.2	335±14	0.03	0.7	1.5
Modified	2 - 4	148790	1.4±0.5	8 ±19	0.9	1.4	2.5
Rayleigh	4 - 8	31270	2.5±1.0	63 ±25	5.5	3.1	4.8
	> 8	12292	5.9±1.6	86 ±16	0.1	4.9	9.4

Table 1: Results of first harmonic analyses in different energy intervals. Data from the regular SD were used above 0.25 EeV, with the East-West method up to 1 EeV and the modified Rayleigh method above 1 EeV. Data from the infill array was used for energies between 0.01 and 0.25 EeV with the East-West method.

ity of only 0.1%. Since several energy bins were searched, these numbers do not represent absolute probabilities. They constitute interesting hints for large scale anisotropies that will be important to further scrutinise with enlarged statistics.

2.3 Upper limits on the dipole

The upper limits on $d_\perp$ at 99%CL are given in Table 1 and shown in Fig. 2, together with previous results from EAS-TOP [7], ICE-CUBE [8] KASCADE [9], KASCADE-Grande [10] and AGASA [11], and with some predictions for the anisotropies arising from models of both galactic and extragalactic cosmic ray origin.

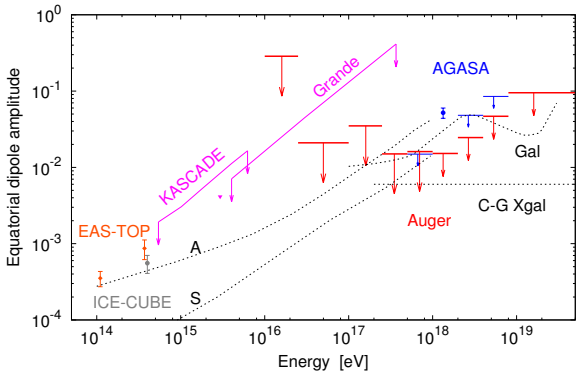

Figure 2: Upper limit at 99%CL for the equatorial dipole amplitude as a function of energy. In red are the limits obtained in this work over the full energy range of the Auger Observatory. Results from AGASA are shown in blue, from KASCADE and KASCADE-Grande in magenta, EAS-TOP in orange and ICE-CUBE in grey. Predictions from different models are displayed, labeled as A, S, Gal and C-G Xgal (see text).

The prediction labeled A and S correspond to a model in wich cosmic rays at 1 EeV are predominantly of galactic origin, and their escape from the galaxy by diffusion and drift motion causes the anisotropies. A and S stand for two different galactic magnetic field symmetries (antisymmetric and symmetric)[12]. In the model labeled Gal [13] a purely galactic origin is assumed for cosmic rays up to the highest energies, and the anisotropy is caused by purely diffusive motion due to the turbulent component of the magnetic field. Some of these amplitudes are challenged by our current bounds. The prediction labeled C-G Xgal [14] is the expectation from the Compton-Getting effect for extragalactic cosmic rays due to the motion of our galaxy with respect to the frame of extragalactic isotropy, assumed to be determined by the cosmic microwave background.

The bounds reported here already exclude the particular model with an antisymmetric halo magnetic field (A) above energies of 0.25 EeV and the *Gal* model at few EeV energies, and are starting to become sensitive to the predictions of the model with a symmetric field.

3 Phase of the first harmonic and prescription

In previous publications of first harmonic analyses in right ascension [5, 15], the Pierre Auger Collaboration reported the intriguing possibility of a smooth transition from a common phase of $\alpha \simeq 270^\circ$ in the first two bins below 1 EeV to a phase $\alpha \simeq 100^\circ$ above 5 EeV. The phase at lower energies is compatible with the right ascension of the Galactic Center $\alpha_{GC} \simeq 268.4^\circ$. It was pointed out that this consistency of phases in adjacent energy intervals is expected with a smaller number of events than the detection of amplitudes standing out significantly above the background noise in the case of a real underlying anisotropy.

This behaviour motivated us to design a prescription with the intention of establishing at 99% CL whether this consistency in phases in adjacent energy intervals is real. Taking advantage of the wide energy range that the Pierre Auger Observatory is capable to scan thanks to the infill array, the test makes use of all data above 10^{16} eV. Thus, once an exposure of 21,000 km^2 sr yr is accumulated by the regular SD array from June 25 2011 on, and applying the same first harmonic analyses described in [5] and performed here [1], a positive anisotropy signal will be claimed within a global threshold of 1% if any, or both, of the following tests succeed:

- Using the infill data, an alignment of phases around the value $\varphi = 263^\circ$ is detected by a likelihood ratio test with a chance probability less than 0.5%, assuming an amplitude signal of 0.5% over the whole energy range analysed.
- Using the regular SD data, an alignment of phases around the curve defined by eq. 4 is detected by the likelihood ratio test with a chance probability less than 0.5%, assuming an amplitude signal comparable to the current mean noise in each energy interval (see Tab. 2).

1. Though a change in the binning for the infill has been made to $\Delta \log_{10}(E) = 0.3$ and a single bin between 17.6< $\log_{10}$(E/EeV)<18.3 because of the low statistics.

$$\varphi(E) = \varphi_0 + \varphi_E \arctan\left(\frac{\log_{10}(E/EeV) - \mu}{\sigma}\right) \qquad (4)$$

To report the midterm status of the prescription, the phase of the first harmonic is shown in Fig. 3. The top panel shows the phase derived with data from January 1 2004 to December 31 2010 for the larger array, that corresponds to the analysis in [5] and from September 12 2007 to April 11 2011 for the infill. The bottom panel is derived with data since June 25 2011 up to December 31, 2012. At this stage, the values as derived from the analysis applied to the infill array are still affected by large uncertainties. On the other hand, the overall behavior of the points as derived from the analysis applied to the regular array shows good agreement with equation 4, using the same parameters as the ones derived with data prior to 2011. The final result of the prescription is expected for 2015, once the required exposure is reached.

ΔE[EeV]	mean noise
0.25 - 0.5	5×10^{-3}
0.5 - 1	5×10^{-3}
1 - 2	3.5×10^{-3}
2 - 4	6.8×10^{-3}
4 - 8	1.4×10^{-2}
> 8	2.0×10^{-2}

Table 2: Mean noise in each energy interval considered in the analysis of the regular array. The analysis performed in the two first energy bins uses the E-W method, which explains why the mean noise is about two times larger than $\sqrt{\pi/N}$.

4 Discussion and conclusions

We have searched for large scale patterns in the arrival directions of events recorded at the Pierre Auger Observatory. No statistically significant deviation from isotropy is revealed within the systematic uncertainties. The probabilities for the dipole amplitudes that are measured to arise by chance from an isotropic flux are of about 0.03% in the energy range from 1-2 EeV, 0.9% for 2-4 EeV and 0.1% above 8 EeV.

These are interesting hints for large scale anisotropies that will be important to further scrutinise with independent data. In addition, the intriguing possibility of a smooth transition from a common phase compatible with the right ascension of the Galactic Center at energies below 1 EeV to a phase around 100° above 5 EeV will be specifically tested through a prescribed test.

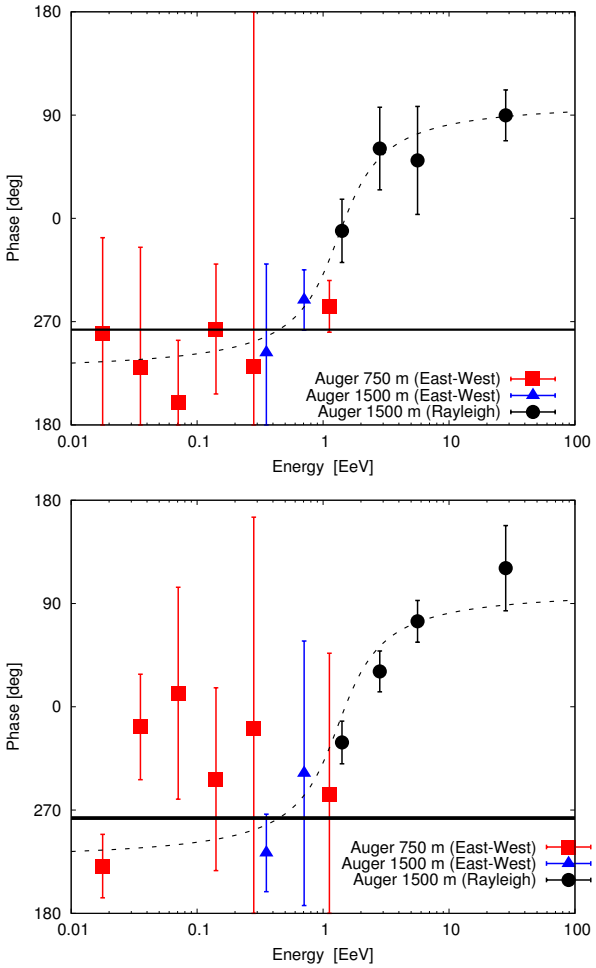

Figure 3: Phase of the first harmonic as a function of energy. The top panel shows the phase calculated using data from January 1 2004 to December 31 2010 for the larger array, and from September 12 2007 to April 11 2011 for the infill. The bottom panel shows the phase derived with data since June 25 2011 up to December 31 2012. The continuous line shown in both plots corresponds to the value φ =263°, that comes from a fit to the phase measured by the infill of the first period, and the dashed line is the fit performed in [5], defined by eq. 4.

References

[1] The Pierre Auger Collaboration, Nucl. Instr. and Meth. A **523** (2004) 50.
[2] I. Mariş, for the Pierre Auger Collaboration, Proc. 32nd ICRC, Beijing, China, **1** (2011) (arxiv:1107.4809).
[3] R. de Almeida, for the Pierre Auger Collaboration, paper 768, these proceedings.
[4] The Pierre Auger Collaboration, Nucl. Instr. Meth. A **613** (2010) 29.
[5] P. Abreu, for the Pierre Auger Collaboration, Astropart. Phys. **34** (2011) 627.
[6] R. Bonino *et al.* Astrophys. J. **67** (2011) 738.
[7] The EAS-TOP Collaboration, Astrophys. J. Lett. **692** (2009) L130.
[8] The ICE-CUBE Collaboration, Astrophys. J. **746** (2012) 33.
[9] The KASCADE Collaboration, Astrophys. J. **604** (2004) 687.
[10] S. Over *et al.* , Proceedings of the 30th International Conference on Cosmic Rays, Merida, **4** (2007) 223.
[11] N. Hayashida *et al.* Astropart. Phys. **10** (1999) 303.
[12] J. Candia, S. Mollerach and E. Roulet, J. Cosmol. Astropart. P. **0305** (2003) 003.
[13] A. Calvez, A. Kusenko and S. Nagataki, Phys. Rev. Lett. **105** (2010) 091101.
[14] M. Kachelriess and P. Serpico, Phys. Lett. B **225** (2006) 640.
[15] The Pierre Auger Collaboration et al., Astrophys. J. **13** (2013) 762.